Vector Velocity Imaging Using Cross-Correlation and Virtual Sources

Voxen, Iben Holfort; Kortbek, Jacob; Jensen, Jørgen Arendt

Published in:
IEEE Ultrasonics Symposium

Link to article, DOI:
10.1109/ULTSYM.2006.517

Publication date:
2006

Document Version
Publisher's PDF, also known as Version of record

In-vivo Vector Velocity Imaging Using Directional Cross-Correlation

Iben Kraglund Holfort[1], Jacob Kortbek[1,2] and Jørgen Arendt Jensen[1]

1) Center for Fast Ultrasound Imaging, Ørsted•DTU,
Build. 349, Technical University of Denmark, DK-2800 Lyngby, Denmark.
2) B-K Medical, Mileparken 34, DK-2730 Herlev, Denmark.

***Abstract*— Previous investigations have shown promising results in using the directional cross-correlation method to estimate velocity vectors. The velocity vector estimate provides information on both velocity direction and magnitude. The direction is estimated by beamforming signals along directions in the range $[0°; 180°[$ and identifying the direction that produces the largest correlation across emissions. An estimate of the velocity magnitude is obtained from the spatial shift between signals beamformed along the estimated direction.**

This paper expands these investigations to include estimations of the vector velocities of a larger region by combining the estimations along several scan lines. In combination with a B-mode image, the vector velocities are displayed as an image of the investigated region with a color indicating the magnitude, and arrows showing the direction of the flow.

Using the RASMUS experimental ultrasound scanner, measurements have been carried out in a water tank using a 7 MHz transducer. A 6 mm tube contained the flow and a Danfoss, MAG 3000, magnetic flow meter measured the volume flow. The tube has a parabolic flow profile with a peak velocity of 0.29 m/s. During the experiments fixed beam-to-flow angles at $\{60°, 75°, 90°\}$ have been applied. The images are obtained using a pulse repetition frequency of 15 kHz, and the images contain 33 lines with 60 emissions for each line.

Corresponding to the three fixed beam-to-flow angles, the angle estimates along the center scan line have a bias of $\{-3.9°, -12.8°, -18.1°\}$ and standard deviation of $\{10.0°, 18.2°, 32.2°\}$. The estimates of the velocity magnitude have bias of $\{4.4\%, 8.1\%, -5.4\%\}$ and standard deviation of $\{9.7\%, 14.3\%, 13.4\%\}$ relative to the peak velocity. The amount of in-tube angle estimates in the range of $\pm 10°$ from the true angle are $\{74\%, 77\%, 66\%\}$.

In-vivo measurements are carried out on a human volunteer. These measurements include the common carotid artery and the femoral bifurcation.

I. Introduction

In conventional blood flow estimation, the velocities are dependent on the direction of the emitted beam, as only the axial component of the velocity vector is estimated. The directional cross-correlation method suggested by Jensen in [1]-[2] is capable of estimating the two-dimensional velocity vector. The two-dimensional velocity vector is independent on the beam direction and provides information on the magnitude as well as the direction of the flow.

In this paper, the directional cross-correlation method is investigated. Based on the theory in [1]-[2], a fully automatic velocity vector estimation algorithm is developed and implemented. Experimental investigations are carried out; these include an experimental setup using a water tank with three different fixed beam-to-flow angles and in-vivo. The in-vivo measurements include the common carotid artery and the femoral bifurcation

II. Velocity Vector Estimation

The two-dimensional velocity vector is obtained by estimating flow direction and velocity magnitude separately as described below.

A. Velocity Estimation

The magnitude of the velocity vector is estimated by identifying the spatial shift of a directional signal over time. Beamforming along the estimated flow direction, two directional signals, $g_1(x')$ and $g_2(x')$, are obtained. Assuming laminar flow, the two directional signals are identical, except for a displacement, due to the movement of the blood scatterers.

The spatial shift between the two signals is found by cross-correlating the two signals

$$\begin{aligned} R_{12}(\tau) &= \frac{1}{L}\int_L g_1(x')\, g_2(x'+\tau)\, dx' \quad (1)\\ &= \frac{1}{L}\int_L g_1(x')\, g_1(x' - |\vec{v}|\, T_{prf} + \tau)\, dx' \\ &= R_{11}(\tau - |\vec{v}|\, T_{prf}), \quad (2)\end{aligned}$$

where L is the length of the directional signal, $R_{11}(\tau)$ and $R_{12}(\tau)$ denote the auto-correlation and the cross-correlation functions, respectively. $R_{12}(\tau)$ is a shifted version of the auto-correlation of the signal $g_1(x')$. The auto-correlation function normally peaks at $\tau = 0$, but due to the subtraction of the term $|\vec{v}|\, T_{prf}$, R_{11} reaches its maximum at $\tau_{peak} = |\vec{v}|\, T_{prf}$. Thus, the magnitude of the velocity vector is found by identifying the lag corresponding to the maximum peak

$$\tau_{peak} = \arg\max_{\tau}\{R_{12}(\tau)\}. \quad (3)$$

The magnitude of the velocity along the flow direction is then

$$|\vec{v}| = \frac{\tau_{peak}}{T_{prf}}, \quad (4)$$

where T_{prf} is the pulse repetition interval.

B. Angle Estimation

The direction of the flow is obtained by estimating the beam-to-flow angle, θ. Based on an assumption of laminar flow, the flow direction provides the largest amount of correlation between the two directional signals. The amount of correlation can be quantified by the correlation coefficient. Let $g_1(x')$ and $g_2(x')$ denote the two directional signals beamformed along the direction, ϕ. By denoting the mean values of each of the signals, μ_1 and μ_2, the correlation coefficient can be estimated by [3]

$$\rho = \max \left\{ \frac{R_{12}(\tau) - \mu_1\mu_2}{\sqrt{[R_{11}(0) - \mu_1^2][R_{22}(0) - \mu_2^2]}} \right\}, \qquad (5)$$

where $R_{11}(0)$ and $R_{22}(0)$ denote the auto-correlation functions at lag 0, and $R_{12}(\tau)$ is the cross-correlation function given by (1). The auto- and cross-correlation functions in (5) are obtained along the direction ϕ.

By beamforming directional signals at angles $\phi \in [0°; 180°[$, the angle estimate can be found from the largest correlation

$$\hat{\theta}_d = \arg\max_{\phi}\{\rho(\phi)\}, \qquad (6)$$

where $\hat{\theta}_d$ is the discrete estimated beam-to-flow angle.

To improve the accuracy of the discrete estimate, $\hat{\theta}_d$, is interpolated using the following expression

$$\hat{\theta} = \hat{\theta}_d - \frac{\rho(\hat{\theta} + \Delta\phi) - \rho(\hat{\theta} - \Delta\phi)}{2(\rho(\hat{\theta} + \Delta\phi) - 2\rho(\hat{\theta}) + \rho(\hat{\theta} - \Delta\phi))}\Delta\phi \qquad (7)$$

where $\Delta\phi$ is the angular distance between two consecutive beamform angles.

III. Measurements

To validate the implemented velocity vector algorithm, a set of measurements have been carried out using the experimental ultrasound scanner, RASMUS [4]. The standard parameters for all measurements are stated in Table I.

A. Experimental Setup

An experimental setup uses a water tank with a tube as illustrated in Fig. 1. The transducer is placed at a fixed beam-to-flow angle, θ, within the water tank. The tube is connected to a pump, and the volume flow rate of the fluid is controlled by a valve and registered by a Danfoss MAG 1100 flow meter. The flow is assumed to be laminar and have a parabolic flow profile, which is characterized by [5]

$$v(z') = v_0 \left(1 - \left(\frac{z'}{R}\right)^2\right), \quad z' \in [-R; R] \qquad (8)$$

where z' denotes the direction perpendicular to the flow direction, R is the radius of the vessel and v_0 is the peak velocity in the center of the vessel. v_0 is determined by the chosen volume flow rate of the pump.

Measurements are carried out using the three beam-to-flow angles, $\theta = \{60°, 75°, 90°\}$, where $\theta = 90°$ is transverse flow.

Type	Linear array
Center frequency, f_0	7 MHz
Pitch of transducer element	208 μm
Height of transducer element	4.5 mm
Kerf	35 μm
Elevation focus	25 mm
Number of transducer elements	128
Apodization, Transmit/Receive	Hamming/None
Number of elements, Transmit/Receive	64 / 64
Excitation pulse, $e(t)$	$\sin(2\pi f_0 t)$
Number of excitation periods	2
Sampling frequency, f_s	40 MHz
Pulse repetition frequency, f_{prf}	15 kHz
Speed of sound, c (in water tank/in-vivo)	1485 m/s / 1540 m/s
Wavelength, $\lambda = c/f_0$ (in water tank/in-vivo)	212 μm / 220 μm
Radius of tube, R	6.0 mm
Peak velocity in flow profile, v_0	0.29 m/s
Volume flow rate, Q	60 l/h
Beam-to-flow angles, θ	$\{60°, 75°, 90°\}$
Depth of focus point, z_f	$\{56, 44, 36\}$ mm
f-number, $f_\#$	$\{4.2, 3.3, 2.7\}$

TABLE I

Standard parameters used in the conducted measurements.

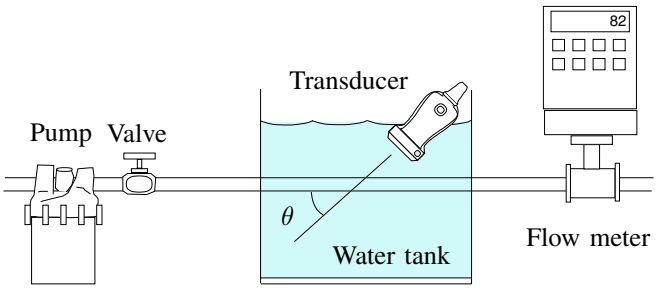

Fig. 1. Illustration of the experimental setup. From [6].

B. Measurement Sequence

The measurements have been carried out using 64 active elements, which are both transmitting and receiving. These 64 elements obtain data, which provides information for one scan line. To obtain data for a full image, the active part of the aperture is displaced along the lateral direction. A total of 33 scan lines with 60 emissions for each line have been acquired resulting in a frame rate of $\simeq 7.5$ Hz.

C. Experimental Validation

The performance of the implemented velocity vector estimation algorithm has been investigated along the center scan line. The performance measures, bias and standard deviation, are stated in Table II. The velocity estimates have been estimated using two different approaches; along the fixed direction, θ, and along the estimated direction, $\hat{\theta}$.

Along the fixed direction, the velocity estimation demonstrates a very satisfying performance for all three test angles, including transverse flow. A decrease in performance, especially for the transverse flow, is identified, when estimating the velocities along the estimated directions. This decrease is a direct consequence of the performance of the angle estimates. Thus, the fully automatic velocity vector estimation algorithm

is limited by the performance of the angle estimation.

Vector flow images have been produced. The velocity vector estimates are visualized using a color to display the magnitude, and an arrow pointing in the direction of the flow. The arrows are scaled by the magnitude of the velocity.

In Fig. 2, the vector flow image of the $\theta = 75°$ measurement is shown. The intensity of the colors and the scaling of the arrows indicate a parabolic flow profile. The general direction of the flow is easily recognized. The distribution of the estimated angles have been investigated. The percentages within $\theta \pm 10°$ are stated in Table III. For all three test angles, the majority of the angle estimates fall within this interval.

θ	$60°$	$75°$	$90°$
Velocity estimates along fixed angles			
B_v	4.39%	8.09%	-5.41%
σ_v	9.66%	14.27%	13.40%
Velocity estimates along estimated angles			
B_v	-3.70%	-11.29%	-25.55%
σ_v	15.12%	18.46%	33.21%
Angle estimates			
B_θ	$-3.91°$	$-12.82°$	$-18.11°$
σ_θ	$10.03°$	$18.24°$	$32.24°$

TABLE II

BIAS AND STANDARD DEVIATION FOR THE VECTOR VELOCITY ESTIMATION ALGORITHMS ALONG THE CENTER SCAN LINE. UNITS ARE IN % RELATIVE TO THE PEAK VELOCITY, v_0, OR IN DEGREES.

θ	$60°$	$75°$	$90°$
$P(\hat{\theta} \in \theta \pm 10°)$	74.33%	77.35%	66.03%

TABLE III

PERCENTAGE OF IN-TUBE ANGLE ESTIMATES WITHIN $\theta \pm 10°$.

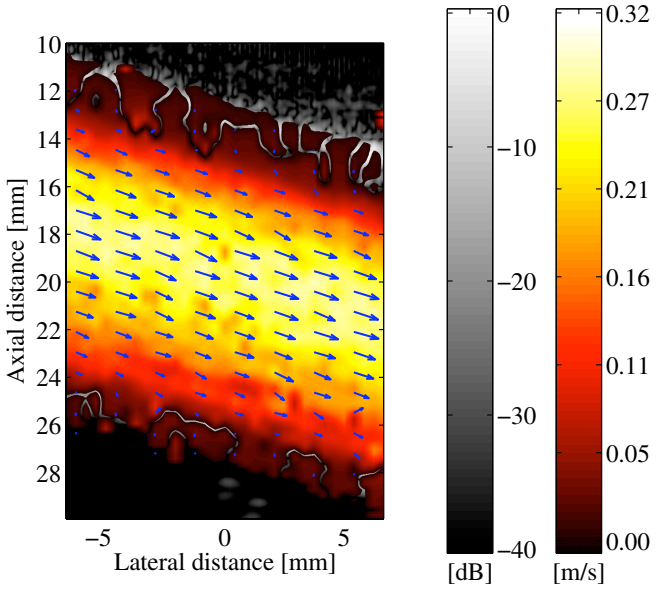

Fig. 2. Vector flow image of the $\theta = 75°$ measurement.

IV. IN-VIVO MEASUREMENTS

Measurements have been carried out on a human volunteer. All measurements are from a healthy 25-year-old female volunteer. The measurements have investigated the blood flow in the common carotid artery and the femoral bifurcation.

Prior to the in-vivo blood flow measurements, the intensities of the actual measurement sequence have been measured. This is a requirement to accommodate the restriction [7] set by the U.S. Food and Drug Administration (FDA). The measured intensities are $I_{spta.3} = 39$ mW/cm^2, $I_{sppa.3} = 9$ W/cm^2 and $MI = 0.14$, which all are well within FDA limits.

For each of the measurements, a sequence of 28 vector flow images have been acquired. These have been combined into movies visualizing the pulsating blood flow in the two arteries. In the following, two single frames from the two movies are shown.

A. Common Carotid Artery

The two vector flow images, Fig. 3, visualize the blood flow in the common carotid artery. In both vector flow images, the general direction of the flow is easily recognized, and the velocities fall in the range of $[0; 0.5]$ m/s.

To estimate the cardiac cycle, the variation of the mean velocity as shown in Fig. 4 is investigated. Each point represents a frame in the acquired sequence. The peak systoles are easily recognized. However, due to the sparse representation, the peak systoles cannot be regarded as more than indications. As a consequence, the first peak has not been acquired. This peak is indicated by the dashed curve.

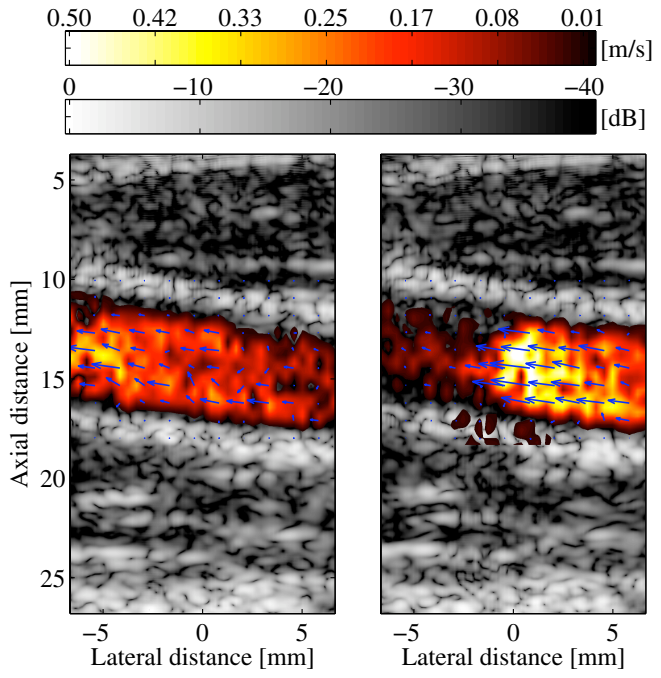

Fig. 3. Vector flow images of the blood flow in the common carotid artery. The two images correspond to peak systoles in the cardiac cycle, and they are acquired at $t = 0.54$ s (left) and $t = 1.74$ (right).

Based on the estimated cardiac cycle, a heart rate of 89.5 bpm is estimated from the time difference between two peaks. Again, due to the sparse representation, the heart rate is merely a rough estimate. The resting normal heart rate is 60-80 bpm [8]. The measured rate is somewhat high, which could be due to stress during the measurement sequence.

The mean blood flow velocity during the systole and diastole in the greater arteries is in the range of 5-18 cm/s [8]. The temporal mean velocity during the entire cardiac cycle is 9.7 cm/s and indicated by the horizontal dashed line in Fig. 4.

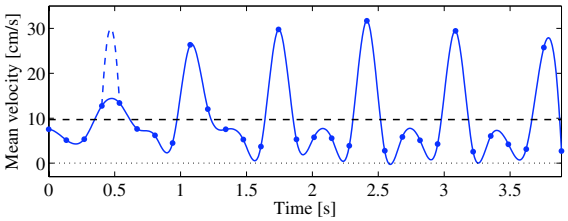

Fig. 4. Variation of the mean velocity in the common carotid artery.

B. Femoral Bifurcation

The estimated blood flow in the femoral bifurcation is visualized by the two vector flow images in Fig. 5. In general, the estimated mean velocities in the femoral arteries are somewhat lower than in the common carotid artery. There are several explanations for this phenomenon, e.g., the reduction of the hydrostatic pressure in the vessels due to a supine position of the test subject.

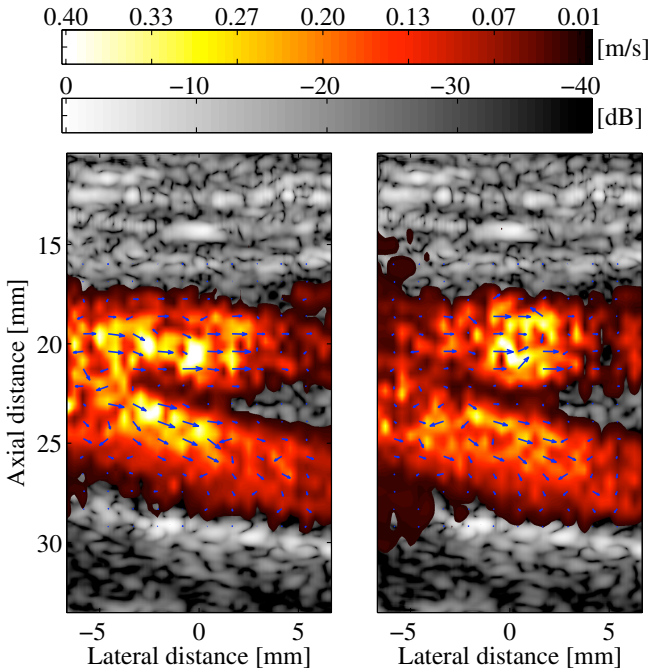

Fig. 5. Vector flow images of the blood flow in the femoral bifurcation. The two images correspond to peak systoles in the cardiac cycle.

The estimated direction of the flow is not as distinct as in the previous measurement. The majority of the angle estimates indicate the direction of the flow from the bifurcation point into the two branches. However, several angle estimates are not consistent with the assumed flow direction. Especially in the deep branch, the angle estimates appear underestimated.

In [9], investigations of the blood flow in the carotid bifurcation using the Transverse Oscillation method have shown a turbulent flow pattern at the bifurcation point and in the internal carotid artery. The turbulent behavior is not evident in Fig. 5. However, this could explain the less distinct flow direction.

V. Conclusions

Based on the theory of the directional cross-correlation method, a fully automatic velocity vector estimation algorithm has been developed and implemented in Matlab. The algorithm has been validated against measurements using an experimental setup. The validation has provided satisfying performance measures. In-vivo measurements have been carried out on a human volunteer for the common carotid artery and the femoral bifurcation. Based on these measurements, vector flow images and movies have been produced.

Acknowledgment

This work was supported by grant 9700883, 9700563 and 26-04-0024 from the Danish Science Foundation and by B-K Medical A/S.

References

[1] J. A. Jensen. Directional velocity estimation using focusing along the flow direction: I: Theory and simulation. *IEEE Trans. Ultrason., Ferroelec., Freq. Contr.*, pages 857–872, 2003.

[2] J. A. Jensen. Velocity vector estimation in synthetic aperture flow and B-mode imaging. In *IEEE International Symposium on Biomedical imaging from nano to macro*, pages 32–35, 2004.

[3] J. S. Bendat and A. G. Piersol. *Engineering Applications of Correlation and Spectral Analysis*. John Wiley & Sons, New York, 2nd edition, 1993.

[4] J. A. Jensen, O. Holm, L. J. Jensen, H. Bendsen, S. I. Nikolov, B. G. Tomov, P. Munk, M. Hansen, K. Salomonsen, J. Hansen, K. Gormsen, H. M. Pedersen, and K. L. Gammelmark. Ultrasound research scanner for real-time synthetic aperture image acquisition. *IEEE Trans. Ultrason., Ferroelec., Freq. Contr.*, 52 (5):881–891, May 2005.

[5] J. A. Jensen. *Estimation of Blood Velocities Using Ultrasound: A Signal Processing Approach*. Cambridge University Press, New York, 1996.

[6] J. A. Jensen and R. Bjerngaard. Directional velocity estimation using focusing along the flow direction: II: Experimental investigation. *IEEE Trans. Ultrason., Ferroelec., Freq. Contr.*, pages 873–880, 2003.

[7] FDA. Information for manufacturers seeking marketing clearance of diagnostic ultrasound systems and transducers. Technical report, Center for Devices and Radiological Health, United States Food and Drug Administration, 1997.

[8] A. Despopoulos and S. Silbernagl. *Color Atlas of Physiology*. Thieme, 1986.

[9] J. Udesen. *2-D blood vector velocity estimation using a phase shift estimator.* PhD thesis, Ørsted•DTU, Technical University of Denmark, 2800, Lyngby, Denmark, 2005.